JOURNAL OF VIROLOGY, July 1996, p. 4683–4690 Vol. 70, No. 7
0022-538X/96/$04.00+0

Murine Coronavirus Membrane Fusion Is Blocked by Modification of Thiols Buried within the Spike Protein

THOMAS M. GALLAGHER*

Department of Microbiology and Immunology, Loyola University Medical Center, Maywood, Illinois 60153-5500

Received 20 December 1995/Accepted 8 April 1996

The envelopes of murine hepatitis virus (MHV) particles are studded with glycoprotein spikes that function both to promote virion binding to its cellular receptor and to mediate virion-cell membrane fusion. In this study, the cysteine-rich spikes were subjected to chemical modification to determine whether such structural alterations impact the virus entry process. Ellman reagent, a membrane-impermeant oxidizing agent which reacts with exposed cysteine residues to effect covalent addition of large thionitrobenzoate moieties, was incubated at 37°C with the JHM strain of MHV. Relative to untreated virus, 1 mM Ellman reagent reduced infectivity by 2 $\log_{10}$ after 1 h. This level of inhibition was not observed at incubation temperatures below 21°C, suggesting that virion surface proteins undergo thermal transitions that expose cysteine residues to modification by the reagent. Quantitative receptor binding and membrane fusion assays were developed and used to show that Ellman reagent specifically inhibited membrane fusion induced by the MHV JHM spike protein. However, this inhibition was strain specific, because the closely related MHV strain A59 was unaffected. To identify the basis for this strain specificity, spike cDNAs were prepared in which portions encoded either JHM or A59 residues. cDNAs were expressed with vaccinia virus vectors and tested for sensitivity to Ellman reagent in the fusion assays. The results revealed a correlation between the severity of inhibition mediated by Ellman reagent and the presence of a JHM-specific cysteine (Cys-1163). Thus, the presence of this cysteine increases the availability of spikes for a thiol modification that ultimately prevents fusion competence.

Virus-induced membrane fusion is an essential step in the entry of enveloped viruses into host cells. Fusion is facilitated by the integral membrane glycoproteins of virions. After the virus binds to the host cell, these fusion proteins undergo structural rearrangements to reveal the hydrophobic character required for lipid mixing and eventual fusion (9, 40). X-ray crystallography results have now shown that the fusion process can be achieved by quite different protein structures; the hemagglutinin trimer of influenza virus projects sharply from the virion and has abundant alpha helicity (43), while the recently resolved E protein of tick-borne encephalitis virus lies flat on the virion surface as a dimer that is rich in beta strands (30). Such findings underscore the importance of examining structure-function relationships in a variety of proteins to provide general principles explaining how fusion is promoted.

This report focuses on the structure and function of the murine coronavirus spike (S) protein, which projects from enveloped virions to mediate both binding to the cell receptor and subsequent virion-cell membrane fusion. The spike is an oligomer (7, 8) that extends 20 nm from the virion envelope (6). In most murine hepatitis virus (MHV) strains, a basic amino acid sequence present within each spike subunit serves as an intracellular proteolytic cleavage site to produce peripheral and integral membrane fragments, designated S1 and S2, respectively (4). Peptide fragments representing peripheral S1 can bind to the MHV receptor (MHVR) (39), thus implicating this fragment in binding. S2 from bovine coronavirus, if expressed in abundance from baculovirus vectors, can decorate cell surfaces and can cause fusion with nearby cells (44), apparently in a receptor-independent manner. Together these findings provide a quite reasonable view of S1 as a receptor-binding entity and S2 as a fusion protein. Complementing this view are molecular genetic results in which cDNAs encoding spikes are mutagenized and then expressed to correlate alterations in primary sequence with membrane fusion function (17). These findings have shown that residues critical for optimal fusion function lie within the S2 fragment, but they have not yet revealed a clear model of how the spike mediates fusion.

Additional biochemical studies of Sturman et al. (36) have advanced our understanding of spike-mediated membrane fusion by establishing fundamental structure-function correlations. In the studies, S1 release from S2 and concomitant S2 aggregation were observed under conditions at which fusion activity was maximal. Because these structural transitions were enhanced in the presence of dithiothreitol, it was suggested that disulfide rearrangements were required during the process. That these findings might be generally relevant to virus-induced membrane fusion was suggested by recent reports showing that agents interfering with thiol-disulfide interchange inhibit both human immunodeficiency virus and Sindbis virus fusion function (1, 32). Thus it became imperative to consider whether fusion induced by the murine coronavirus spike is sensitive to thiol modification.

The spikes of murine coronaviruses are cysteine rich; in strain JHM, the ectodomain portion of each subunit contains 49 cysteines (29). While most of these cysteines are likely involved in intrasubunit disulfide bonding (28), it is shown here that at least one is available for modification by a membrane-impermeant thiol blocker, Ellman reagent. This is because Ellman reagent specifically blocks spike-mediated membrane fusion. This blockade depends in part on the presence of a cysteine residue (Cys-1163) in the S2 ectodomain. These findings help to pinpoint a critical step in the adoption of fusion competence by the large spike glycoprotein.

* Mailing address: Department of Microbiology and Immunology, Loyola University Medical Center, 2160 S. First Ave., Maywood, IL 60153-5500. Phone: (708) 216-4850. Fax: (708) 216-9574. Electronic mail address: tgallag@luc.edu.

MATERIALS AND METHODS

Cells. Monolayer cultures of murine 17c11 fibroblasts (37) were grown in Dulbecco's modified Eagle medium (DMEM) supplemented with 5% tryptose phosphate broth (Difco Laboratories, Detroit, Mich.) and 5% heat-inactivated fetal calf serum (ΔFCS; Gibco Laboratories, Grand Island, N.Y.). Murine delayed brain tumor (DBT) cells (21) were grown in minimal essential medium supplemented with 10% tryptose phosphate broth and 5% ΔFCS. Rabbit kidney (RK13) and HeLa cells were grown in DMEM containing 10% ΔFCS. All growth media contained 0.01 M sodium HEPES (*N*-2-hydroxyethylpiperazine-*N*′-2-ethanesulfonic acid [pH 7.4]).

Growth, purification, and analysis of MHVs. MHV strains A59, JHMX, and MHV4 were inoculated onto 17cl1 cell monolayers in serum-free DMEM (SFM) for 1 h at 37°C and then replaced with DMEM containing 2% ΔFCS and incubated at 37°C for 12 to 16 h, at which time considerable cytopathology was evident in all cells. Virions were collected from culture supernatants and immediately purified by differential centrifugation. In brief, debris was removed by sequential spins (10 min, 2,000 × *g*, 5°C, and then 30 min, 10,000 × *g*, 5°C). To prepare virions for fusion assays, the clarified supernatants, typically 20 ml, were incubated at 37°C in the presence or absence of 1 mM Ellman reagent (Pierce Co., Rockford, Ill.) and then overlaid on 30% (wt/wt) sucrose cushions (10 ml) in HNB buffer (25 mM sodium HEPES [pH 7.4], 100 mM NaCl, 0.01% bovine serum albumin [BSA]). A 6-ml cushion of 50% (wt/wt) sucrose in HNB buffer was underlaid, and virions were sedimented in the Beckman-Spinco SW28 rotor at 5°C for 3 h at 28,000 rpm. Virions were collected from the interface between the 30 and 50% sucrose solutions by fractionation and stored at −80°C. The titers of virus preparations were determined by plaque assay on DBT cell monolayers.

Electrophoresis of virion proteins was carried out on discontinuous polyacrylamide (Laemmli) gels, as described previously (18). Prior to loading, samples were mixed with equal volumes of a modified solubilizer solution adjusted to a pH of 4.0 (0.125 M sodium citrate [pH 4.0], 5% Ficoll, 4% sodium dodecyl sulfate [SDS], 0.01% bromphenol blue) and heated for 5 min at 100°C. Reducing solubilizer contained 10% 2-mercaptoethanol. After electrophoresis, proteins were transferred to nitrocellulose membranes, and the position of the S2 fragments was identified by immunoblotting with rabbit anti-S2 peptide antiserum 3300, as described previously (18).

Virion-receptor binding assay. Direct measurement of virion adsorption to receptor-bearing cells required abundant receptor levels on the plasma membrane. Therefore, receptors were overexpressed with vaccinia virus vectors. To prepare the vectors, a cDNA encoding the primary MHVR was obtained by reverse transcriptase PCR (22, 23) of BALB/c mouse liver RNA, with primers based on the reported MHVR sequence (10). MHVR-encoding cDNA was then inserted into vaccinia virus insertion/expression plasmid pTM3 (12, 26) between the *Nco*I and *Spe*I sites of the polylinker. The resulting pTM3-MHVR was transfected into HeLa cells infected 1 h earlier with vaccinia virus WR. Transfection was mediated by Lipofectin reagent (Gibco BRL, Gaithersburg, Md.) and was performed according to the manufacturer's instructions. At 3 days post-vaccinia virus infection, progeny virus was collected by freezing and thawing and then plated on RK13 cell monolayers. Plaques representing amplified recombinant vaccinia virus were selected by subjecting the cells to mycophenolic acid exposure as previously described by Falkner and Moss (13). Virus from well-isolated plaques was amplified in HeLa cells to generate stocks of recombinant virus, designated vTM3-MHVR.

Negative controls in virion-receptor binding assays required construction of a second vaccinia virus recombinant which harbored a form of MHVR cDNA with a deletion and was therefore unable to express virus binding determinants. This was prepared similarly to that described previously by Dveksler et al. (11). In brief, pTM3-MHVR was used as the template for a series of PCRs involving primers capable of amplifying the 5′ 148 bp and the 3′ 929 bp of the 1,377-bp MHVR open reading frame. Engineered into the relevant primers were sites for *Xma*I digestion. This permitted ligation of the two PCR DNAs after each was digested with *Xma*I, thereby generating an in-frame deletion. cDNA was then inserted back into the pTM3 vector, and the recombinant virus was prepared as described above. Receptor protein expressed from this recombinant lacked residues 11 to 122; this amounts to the bulk of the amino-terminal (virus binding) domain (NTD). The recombinant virus was designated vTM3-MHVR$_{\Delta NTD}$.

Expression of the receptor glycoproteins was accomplished by coinfection of HeLa cells with vTF7.3, which encodes T7 RNA polymerase (15), and with vTM3-MHVR at equivalent multiplicities of infection. Synthesis of the receptor glycoproteins was monitored by immunoblot assays of cell lysates as described elsewhere (16).

In virion-receptor binding assays, HeLa cell monolayers were rinsed with SFM at 16 h post-vaccinia virus infection, and then [^{35}S]Met- and/or Cys-labelled MHV particles in SFM were incubated for 2 h at 4°C. Unadsorbed virions were then removed, cells were rinsed five times with ice-cold phosphate-buffered saline (PBS) containing 0.05% Tween 20 and 0.5% BSA, and lysed in radioimmunoprecipitation assay buffer (0.01 M Tris-HCl [pH 7.2], 0.15 M NaCl, 1% sodium deoxycholate, 1% Triton X-100, 0.1% SDS). Radioactivity associated with the media and the cell lysates was quantified by scintillation counting and was expressed as the percentage associated with the cells.

Construction of HeLa cells expressing MHVR. Fusion assays involved the use of human (HeLa) cell lines that have been stably transfected with cDNA encoding the MHVR. Briefly, PCR-amplified MHVR cDNA was inserted into expression plasmid pUHD10-3 (19), and then the construct was transfected by lipofection into subconfluent HeLa-tTA cells (19) in conjunction with a 10-fold molar excess of pSV2-GPT (Clontech, Palo Alto, Calif.). pSV2-GPT encodes *Escherichia coli* guanosine phosphoribosyltransferase (GPT) and thereby confers resistance to mycophenolic acid. GPT-positive clones were selected by long-term (3-to-4-week) growth in DMEM–5% ΔFCS containing 2.5 μg of mycophenolic acid per ml, 250 μg of xanthine per ml, and 20 μg of hypoxanthine per ml. After selection and subcloning, surface expression of the MHVR was confirmed in a number of clones by indirect immunofluorescence with murine antireceptor antibody CC1 (42) and fluorescein isothiocyanate-conjugated goat antibody directed against mouse immunoglobulin (Cappel, Inc., Durham, N.C.). Clones were designated as HeLa-MHVR transfectants.

Virion-cell fusion assay. HeLa-MHVR cells were divided into two identical 75-cm^2 monolayer cultures. One culture was coinfected with vaccinia virus recombinants vTF7.3 and vTM1-MHVR, while the other was infected with the wild-type vaccinia virus strain WR and then transfected by lipofection with plasmid pG1NT7-βgal. pG1NT7-βgal is a plasmid which carries a gene for β-galactosidase under the transcriptional control of a T7 promoter and was made available for this study by Richard A. Morgan, National Center for Human Genome Research, Bethesda, Md. At 6 h postinfection, cells in each culture were suspended by trypsinization, mixed, and diluted to 10^6 cells per ml in DMEM–10% ΔFCS. One-milliliter aliquots were replated onto 5-cm^2 tissue culture wells. After allowing 1 h at 37°C for the resettling of the cells, sucrose gradient-purified virions (in HNB buffer containing 40% sucrose) were diluted fivefold in SFM and added directly to the wells at 37°C. The input multiplicities were 10 (JHMX) and 50 (A59) PFU per cell. At 1 h post-virion addition, ΔFCS was added to the wells to a final concentration of 5%. At 1, 2, and 3 h post-virion addition, cells were rinsed with PBS and lysed with 0.5 ml of PBS per well containing 0.5% Nonidet P-40. The quantity of β-galactosidase in each lysate was measured by the colorimetric assay described previously (27) and normalized by comparison of substrate hydrolysis produced by a standard preparation of *E. coli* β-galactosidase (Calbiochem, La Jolla, Calif.). Values were expressed as nanograms of β-galactosidase per unit volume of cell lysate.

Mutagenesis of spike-encoding cDNAs. Plasmid DNA pGEM4Z-S$_{WT}$, encoding the complete spike protein of MHV4, has been described previously (17) and hereinafter will be designated pGEM4Z-S$_4$. To convert cysteine codon 1163 within the spike open reading frame to tyrosine, a mutagenic oligomer was synthesized which represented nucleotides 3463 to 3495 (numbering here and throughout text is according to reference 29) and which harbored TAT (tyrosine codon) in place of the wild-type TGT (cysteine codon) at nucleotides 3487 to 3489. This oligomer (50 pmol), an equimolar amount of SP6 promoter/primer (Promega Corp., Madison, Wis.), and 10 ng of pGEM4Z-S$_4$ template were used in a standard PCR (22) to produce the desired 726-bp DNA fragment. The PCR DNA was purified on adsorbent resin (Promega Corp.), digested with *Bsm*I and *Xba*I, gel purified, and ligated directly to the gel-purified 6.2-kbp *Bsm*I-*Xba*I fragment of pGEM4Z-S$_4$. The resulting plasmid DNA, pGEM4Z-S$_4$ (C-1163→Y [C1163Y]), was amplified and purified and then sequenced by the chain termination method to confirm the introduction of the desired mutation. Cloning and sequencing steps were done according to protocols described in laboratory manuals (33).

To convert the majority of the S2-encoding region of S$_4$ cDNA to strain A59 sequences, PCR was again employed. Briefly, total cellular RNA was extracted from MHV A59-infected 17cl1 cells (18), and S2 sequences were amplified by reverse transcriptase PCR (23) with PCR primers identical to nucleotides 2302 to 2321 and complementary to nucleotides 4140 to 4159. The resultant 1,857-bp PCR DNA was purified and digested with *Sph*I and *Nde*I to generate a 1,422-bp restriction fragment, which was gel purified and ligated to the larger 8.3-kbp fragment resulting from a parallel *Sph*I and *Nde*I digestion of pTM1-S$_4$. The exchange resulted in pTM1-S1$_4$S2$_{A59}$, and sequencing confirmed the replacement of codons 785 to 1256 of S$_4$ with S$_{A59}$. Thus, this plasmid encoded a spike containing a tyrosine residue at position 1163. To convert this tyrosine codon to cysteine, mismatch oligonucleotides were synthesized and employed in PCRs analogous to that described for construction of the C1163Y mutant. This permitted construction of pTM1-S1$_4$S2$_{A59}$ (Y1163C).

Vaccinia virus-based spike protein expression. Transient expression of the various MHV spike proteins in HeLa tTA cells was performed as described previously (17). Confluent monolayers of cells grown on 24-well (2 cm^2 per well) cluster plates were infected with recombinant vaccinia virus vTF7.3, which expresses T7 RNA polymerase (15). After 1 h at 37°C, inoculum virus was removed, cells were rinsed three times with SFM, and plasmid DNA-Lipofectin complexes (0.5 μg of DNA–2.5 μg of Lipofectin in 0.2 ml of SFM) were added to each well. At 5 h posttransfection, the complexes were removed and DMEM–10% ΔFCS was added.

Cell-cell fusion assay. At 16 h posttransfection, the spike-expressing HeLa-tTA cells were rinsed once with cysteine-deficient DMEM and then overlaid with 0.4 ml (per well) of the same medium containing 0.1 μg of brefeldin A (Sigma Chemicals, St. Louis, Mo.) per ml. Identical wells then immediately received 0.04 ml of 0.1 M sodium phosphate (pH 8.0) or 0.04 ml of 10 mM Ellman reagent in

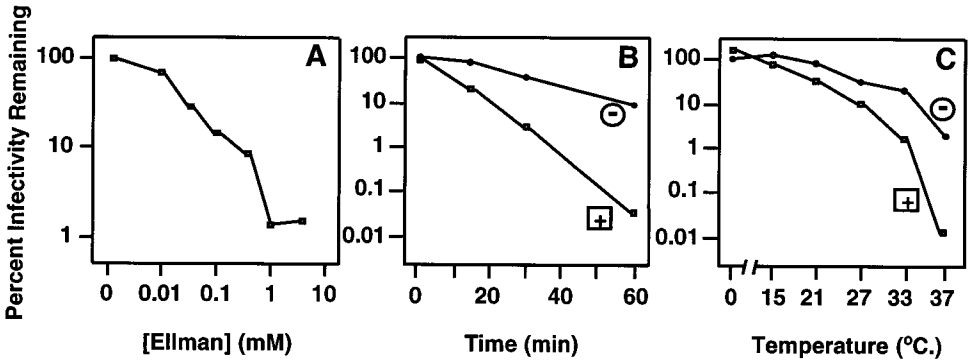

FIG. 1. Effect of Ellman reagent on MHV4 (JHM) infectivity. Virus at 10^6 to 10^7 PFU/ml was incubated under the conditions indicated in complete growth medium and then serially diluted in ice-cold serum-free medium and plated on DBT indicator cells for plaque development. Plaques were scored after a 3-day incubation by crystal violet staining. (A) Effect of reagent concentration at 37°C for 1 h; (B) rate of inactivation at 37° by 1 mM reagent; (C) effect of temperature during 1-h exposures to 1 mM reagent. + and − refer to the presence and absence of Ellman reagent, respectively.

the same buffer. Incubation was continued for 1 h at 37°C prior to addition of receptor-expressing cells.

To prepare indicator cells with which to measure the fusion potency of spikes, one 75-cm^2 monolayer of HeLa-MHVR cells (clone 3) was infected with vaccinia virus strain WR and then transfected with plasmid pG1NT7-βgal (27). At 16 h posttransfection, cells were trypsinized and resuspended in 10 ml of DMEM–10% ΔFCS containing 0.1 μg of brefeldin A per ml. Identical 5-ml volumes of resuspended cells immediately received 0.5 ml of 0.1 M sodium phosphate (pH 8.0) or 0.5 ml of 10 mM Ellman reagent in the same buffer. Aliquots (0.4 ml each) of each cell suspension were then immediately distributed into the appropriate wells containing the pretreated spike-bearing HeLa-tTA cells.

After 2 h at 37°C, at which time all cells had settled and clear evidence of syncytium formation was evident in wells containing spike protein, monolayers were rinsed two times with PBS and then lysed by addition of 0.5 ml (per well) of PBS containing 0.5% Nonidet P-40. The amounts of β-galactosidase in each sample were determined by the colorimetric enzyme assay (27).

RESULTS

Ellman reagent inhibits the infectivity of MHV4 (JHM). Previous reports describing the effect of Ellman reagent on virus entry indicated that the chemical, when used at millimolar concentrations, did not destroy the infectivity of human immunodeficiency virus virions (32) or Sindbis virions (1). In contrast, Ellman reagent, when mixed with MHV4 virions, was potently antiviral (Fig. 1). Reagent (1 mM) reduced the infectious titer of MHV4 by 2 $\log_{10}$ after 1 h at 37°C (Fig. 1A). The inactivation kinetics roughly followed a first-order progression, leading to a 2-$\log_{10}$ infectivity difference between untreated virus and Ellman reagent-treated virus after 1 h at 37°C (Fig. 1B).

The temperature dependence of the process (Fig. 1C) strongly suggested that the spike protein undergoes a thermally induced structural transition to render itself available to inactivation by Ellman reagent. Below 21°C, the reagent exerted only nominal antivirion activity, whereas at 33 and 37°C, the levels of inhibition were 10- and 100-fold, respectively. This was not due to pH elevation and concomitant increased thiol reactivity at the higher incubation temperatures—the pH of the growth medium remained 7.6 ± 0.1 at all tested temperatures. This temperature-dependent inactivation was also not attributable to increased reactivity of Ellman reagent at the higher temperatures, because reaction of the reagent with cysteine generated the characteristic yellow nitrothiobenzoate product (ε_{412} = 14,150 [31]) at equivalent rates throughout the 15 to 37°C range (data not shown).

Mutant forms of MHV4, including variants OBLV (17) and JHMX (29), were found to be similarly inactivated by Ellman reagent. These variants contain point mutations and deletion mutations, respectively, within the spike gene. In dramatic contrast, the infectivity of the related MHV strain, A59, was essentially unaffected by exposure to the reagent. MHV A59 was resistant to inactivation despite the fact that its spike protein shares 92.4% amino acid identity with the strain 4 spike (25, 29).

Ellman reagent does not inhibit virion-receptor binding but does inhibit virion-cell fusion. Since the membrane-impermeant Ellman reagent was thought to modify the protruding spikes, assays capable of monitoring spike function were developed and used to identify the basis for the infectivity reductions. Virion binding assays were initially performed. This involved direct measurement of ^{35}S-labeled virion binding to MHVRs (10) that were overexpressed on cell surfaces. Vaccinia virus recombinants capable of expressing MHVR in abundance were prepared. One recombinant contained a complete cDNA capable of encoding MHVR, while another control recombinant encoded a truncated form lacking the amino-terminal domain (the NTD) that confers virion binding (11). In each case, the cDNAs were juxtaposed near the bacteriophage T7 promoter so that coinfection of the viruses with the T7 RNA polymerase-encoding vaccinia virus vector vTF7.3 would result in abundant receptor mRNA and protein synthesis (14).

Ellman reagent-resistant strain A59 and Ellman reagent-sensitive strain JHMX were chosen for these analyses because, unlike MHV4 (strain JHM), these viruses grow to reasonably high titers in 17cl1 cell culture, and therefore particles could be readily purified and analyzed. Straightforward assays involving adsorption of the purified ^{35}S-labeled virions to HeLa cells showed that the complete MHVR-expressing cells bound about three times more ^{35}S-labeled virus than the cells expressing $MHVR_{\Delta NTD}$ (Table 1). Ellman reagent, which effected a ninefold drop in JHMX infectivity in this experiment, had no measurable effect on the level of ^{35}S-labeled virus adsorption (Table 1). The reagent, therefore, did not block at the receptor binding stage.

To find out whether the virions after exposure to Ellman reagent could still induce membrane fusion, a quantitative virus-cell fusion assay was employed that was modeled after the one described by Nussbaum et al. (27). The assay involved the use of a transfectant HeLa cell line that constitutively expresses the MHVR (Fig. 2 [see schematic depiction]). One population of these cells contained T7 RNA polymerase activity via prior infection with vTF7.3, while another harbored a plasmid encoding β-galactosidase under the transcriptional control of the T7 RNA polymerase promoter. The populations

TABLE 1. Adsorption of virus particles to the MHVR is not impaired by exposure to Ellman reagent

Virus[a]	Ellman reagent[b]	Receptor[c]	% Cell-associated virus[d]
JHMX	+	$MHVR_{\Delta NTD}$	4.1
	−		3.7
	+	MHVR	10.5
	−		10.5
A59	+	$MHVR_{\Delta NTD}$	12.6
	−		12.2
	+	MHVR	33.4
	−		34.0

[a] 10^5 PFU per sample. For JHMX, 10^5 PFU = 8.4×10^4 ^{35}S cpm. For A59, 10^5 PFU = 1.2×10^5 ^{35}S cpm.

[b] Viruses were mixed with equal volumes of PBS (pH 7.1) plus or minus 2 mM Ellman reagent for 1 h at 37°C, and then the mixtures were diluted to 1-ml volumes with ice-cold serum-free DMEM. Plaque assays showed that the exposure to Ellman reagent caused a ninefold decrease in JHMX titer, while A59 titers were unaffected.

[c] Volumes (0.4 ml each) of virus were incubated for 2 h at 4°C on HeLa cell monolayers (5 cm^2) infected 16 h earlier with vaccinia virus recombinants expressing the complete receptor (MHVR) or a control receptor lacking the virus binding domain (ΔNTD).

[d] Radioactivity associated with cells and media was quantified by scintillation counting and expressed as the percentage associated with the cells.

were mixed, and MHV particles were added. Because intercellular fusion directly induced by MHV A59 particles has been reported (35), the expectation was that virion addition to the mixed population would similarly fuse cells and permit transfer of the T7 RNA polymerase to those cells harboring the transcriptionally silent β-galactosidase gene. Since the time required for production of a fusogenic spike by infected cells is greater than 4 h, the β-galactosidase expressed within 4 h of MHV inoculation would serve to measure only the relative fusion potency of the exogenously added virions.

The results of this assay (Fig. 2) clearly revealed that Ellman reagent specifically inhibited JHMX fusion function. While the exogenous addition of untreated JHMX induced increasing synthesis of β-galactosidase from 1 to 2 h, an equivalent number of inactivated Ellman reagent-treated particles was unable to induce β-galactosidase production above the levels observed in control cultures lacking virions. By 3 h, some enzyme activity was evident in cells given the Ellman reagent-treated JHMX, but the level was about 1/10 that induced by untreated virus. In contrast, the level of A59-induced fusion remained low and was not perturbed by Ellman reagent. This minimal fusion by A59 might be due in part to the large proportion of uncleaved S in the preparation, because S cleavage is well known to enhance MHV A59 fusion (35).

Electrophoretic analyses suggest that spikes projecting from strain JHMX virions contain unpaired cysteine(s). Such a clear difference between JHM and A59 viruses in reagent-mediated inhibition suggested that a critical reactive thiol is present in the sensitive JHM strains and that modification of this thiol prevents fusion competence. Indeed, comparison of the primary sequences of JHM and A59 spike proteins revealed a single nonconserved cysteine that was unique to JHM (Fig. 3 [the long hatch mark and the arrow depict the JHM-specific cysteine]). The ectodomain portion of S2 from A59 contains an even-numbered 12 cysteines, with a tyrosine at the corresponding JHM cysteine codon 1163. This odd-numbered 13th cysteine in Ellman reagent-sensitive JHM strains is located in S2 between two putative amphipathic alpha helix domains, about 160 residues from the transmembrane-spanning region.

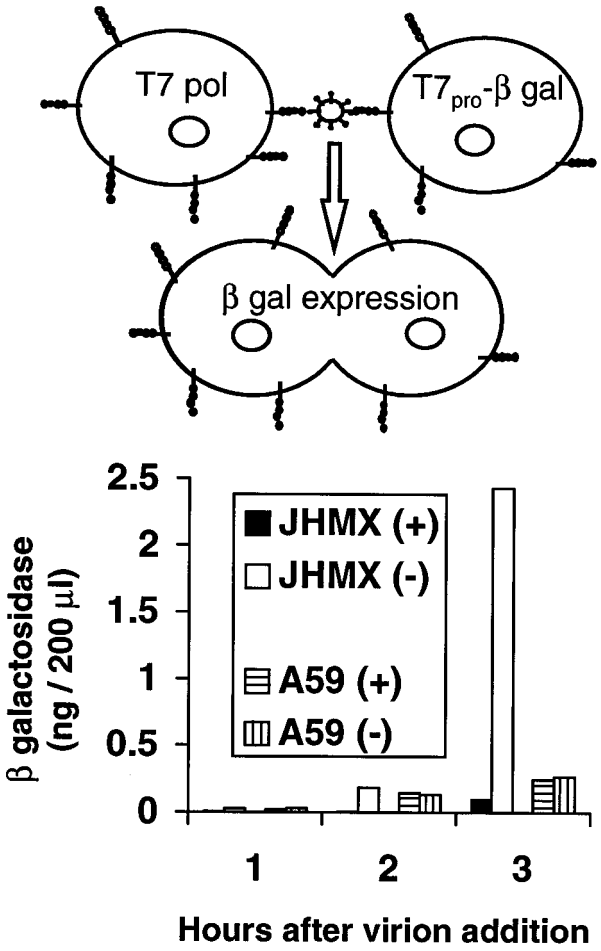

FIG. 2. Effect of Ellman reagent on the ability of virions to mediate intercellular fusion. Receptor-bearing HeLa-MHVR cells (depicted at the top) were divided into two identical cultures. One culture was infected with the vaccinia virus recombinant vTF7.3 to synthesize T7 RNA polymerase within the cells (T7 pol cells; upper left). The other culture was infected with wild-type vaccinia virus strain WR and then transfected with plasmid pG1NT7-βgal, which encodes *E. coli* β-galactosidase ($T7_{pro}$-β gal cells, upper left). At 6 h postinfection, the two cultures were trypsinized, mixed, and replated onto tissue culture wells. One hour later, gradient-purified MHV particles left untreated (−) or treated with Ellman reagent (+) were added directly to the wells at 37°C (virion depicted between cells). At the indicated times after coronavirus addition, cells were rinsed with PBS and lysed with PBS containing 0.5% Nonidet P-40. The amounts of β-galactosidase in each sample were determined by a colorimetric enzyme assay as described in Materials and Methods. β-Galactosidase values obtained in control samples lacking MHV particles were subtracted prior to plotting of the data.

S2 fragments containing an odd number of cysteines might contain thiol(s) available for modification by Ellman reagent, or they might alternatively be engaged in intermolecular disulfide bridging. To find out whether intermolecular disulfides are a component of JHM spike quaternary structure, the proteins of virion preparations were subjected to SDS-polyacrylamide gel electrophoresis (PAGE) under nonreducing and reducing conditions. Because the electrophoretic analyses of MHV virion proteins are typically hampered by the formation of SDS-resistant spike aggregates, samples were prepared by adjusting SDS solubilization buffers to a low pH of 4.0 instead of the usual more neutral pH solubilization conditions.

Samples prepared in this way yielded interpretable profiles. Under nonreducing conditions, immunoblots revealed a small proportion of S2-specific protein at a ca. 180-kDa position and

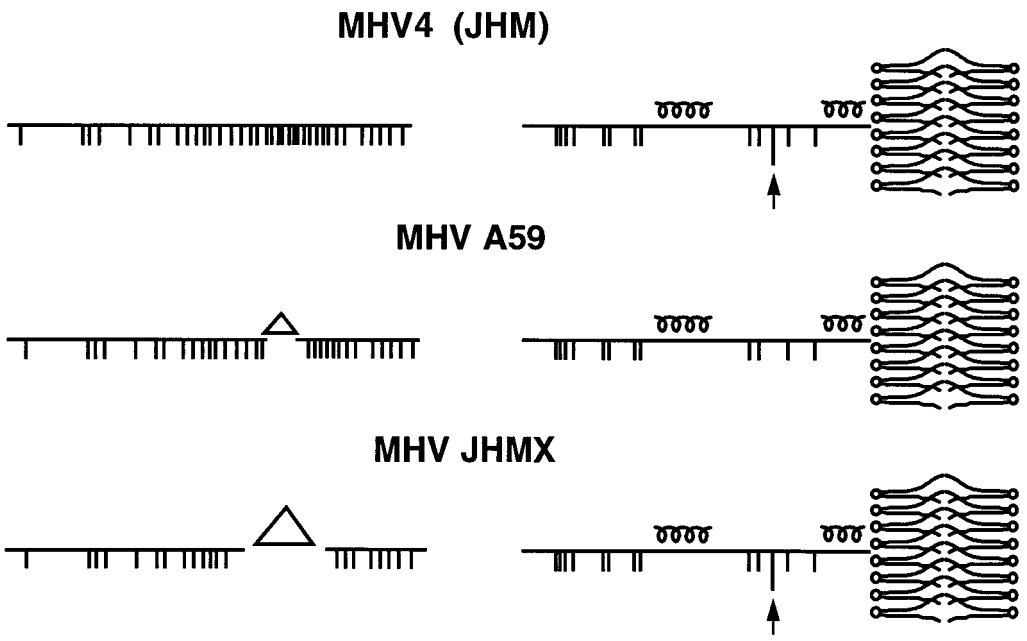

FIG. 3. Distribution of cysteine residues on spike ectodomains. Spike ectodomains (MHV4; 1,320 residues, MHV A59; 1,268 residues, MHV JHMX; 1,167 residues) are depicted by two horizontal lines. The left line represents the peripheral S1 fragment, while the right line (embedded in the membrane) represents the integral S2 chain. The triangles illustrate deletions within S1. Squiggles above each S2 chain designate regions predicted as amphipathic helix (7). Hatch marks perpendicular to each chain show the positions of cysteine residues. The single longer hatch mark (arrows) between the predicted helices of S2 represents the single cysteine (Cys-1163) that is unique to MHV4 and JHMX spikes. Each spike monomer also contains 56 residue transmembrane and cytoplasmic domains (not depicted) which are highly conserved and contain 10 cysteine residues.

a relatively larger amount of 90-kDa monomeric S2 (Fig. 4). That the 180-kDa form represented some disulfide-linked S2 was shown by the parallel immunoblot of reduced JHMX proteins (Fig. 4). Thus, while a small proportion of the JHMX spike exhibited an intermolecular disulfide arrangement, the majority of the unreduced JHMX S2 chains remained monomeric and so are liable to contain free thiols.

Spikes with an odd number of cysteines in the S2 ectodomain are sensitive to fusion inactivation by Ellman reagent. The role of an odd-numbered, unpaired cysteine as a target for Ellman reagent was first investigated by synthesizing and analyzing the fusion function of a site-directed mutant form of the MHV4 (strain JHM) spike protein. The MHV4 spike cDNA, designated S_4, was mutated as described in Materials and Methods to change the cysteine codon at position 1163 to the A59-specific tyrosine. The mutant was designated S_4 (C1163Y). Spikes were expressed from cDNAs in vTF7.3-infected HeLa cells, and their fusion potency was quantitated in the presence and absence of Ellman reagent. To this end, spike-bearing cells were incubated for 1 h at 37°C with or without Ellman reagent prior to overlay of receptor-bearing target cells loaded with the reporter β-galactosidase gene. Spike fusion function was measured 2 h after overlay of target cells by measurement of β-galactosidase enzyme activity.

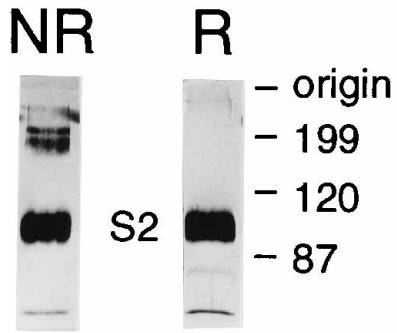

FIG. 4. Electrophoretic behavior of JHMX S2 fragments under nonreducing (NR) and reducing (R) conditions. Gradient-purified JHMX particles (10^6 PFU in 10 μl) were subjected to SDS-PAGE as described in Materials and Methods. S2 chains were then identified by immunoblotting (18). Molecular mass markers in kilodaltons are indicated on the right.

These fusion assays differed from the virion-cell fusion assays described above in that spikes were continuously expressed within cells. They also differed in that initial tests revealed that fusion could not be readily inhibited—at best, the Ellman reagent provided only a 30% reduction of β-galactosidase activity (data not shown). This failure of the reagent to dramatically inhibit fusion was attributed to constitutive spike expression. Indeed, the possibility that spikes reaching the cell surface might be able to induce fusion faster than Ellman reagent could inactivate them was suggested by the fact that JHM virions were only slowly inactivated (Fig. 1B). Thus, to restrict the analysis to previously transported spikes, Ellman reagent was tested in the presence of 0.1 μg (per ml) of brefeldin A, a general inhibitor of protein transport through the secretory pathway (24). This critical addition of brefeldin A increased the inhibitory effect of Ellman reagent significantly, presumably because it restricted the requirement for inactivation to previously transported spikes.

Once developed, the fusion tests revealed that the conversion of cysteine 1163 to tyrosine changed spike function in two ways (Table 2). First, the conversion reduced fusion potency by about 80%. Second, the conversion reduced the sensitivity to reagent-mediated inhibition about twofold. Thus, the presence of cysteine 1163 enhances fusion and is also required to achieve maximal inhibition by the Ellman reagent.

TABLE 2. C1163Y change in the MHV4 spike protein (S_4) increases resistance to Ellman reagent

Plasmid[a]	β-Galactosidase activity (ng/50 μl)[b]		% Inhibition[c]
	+ Ellman reagent	− Ellman reagent	
pTM1 (no S) (negative control)	0.046	0.051	
pGEM4Z-S_4 1	0.832	2.45	67
pGEM4Z-S_4 2	0.248	2.03	90
pGEM4Z-S_4 3	0.330	1.08	72
pGEM4Z-S_4 (C1163Y) 1	0.128	0.210	48
pGEM4Z-S_4 (C1163Y) 2	0.218	0.368	46
pGEM4Z-S_4 (C1163Y) 3	0.180	0.260	36
pG1NT7-βgal (positive control)	6.86	7.09	3

[a] HeLa-tTA cells (2 cm^2) were infected with recombinant vaccinia virus vTF7.3 and then transfected by lipofection with 1 μg of the indicated plasmid DNAs.

[b] At 16 h posttransfection, cells were rinsed and incubated for 1 h at 37°C in 0.5 ml (per well) of serum-free medium containing 0.1 μg of brefeldin A per ml, plus or minus 1 mM Ellman reagent. Fusion potential of spikes was then measured by addition of 0.5 ml (per well) of complete medium containing 2×10^5 HeLa-MHVR cells that had been infected/transfected 16 h earlier with vaccinia virus strain WR/pG1NT7-βgal. After allowing 2 h at 37°C for the spike and receptor-bearing cells to fuse, monolayers were rinsed with PBS and lysed in PBS containing 0.5% Nonidet P-40. The amount of β-galactosidase in 50-μl aliquots was measured by a colorimetric enzyme assay.

[c] Percent inhibition =

$$(100)1 - \frac{(\beta\text{-galoctosidase} - \beta\text{-galactosidase}_{\text{Negative control}}) \text{ in presence of reagent}}{(\beta\text{-galactosidase} - \beta\text{-galoctosidase}_{\text{Negative control}}) \text{ in absence of reagent}}$$

To determine whether the reciprocal conversion of tyrosine to cysteine in the A59 S2 fragment would increase sensitivity to Ellman reagent, additional spike cDNA clones were constructed. One encoded a hybrid spike in which residues comprising the S2 ectodomain were identical to MHV A59. This clone was designated $S1_4$:$S2_{A59}$. The other was obtained after site-directed mutagenesis of the tyrosine at position 1163 to cysteine ($S1_4$:$S2_{A59}$ [Y1163C]). Spikes from these cDNAs induced intercellular membrane fusion to similar levels. However, the presence of the cysteine about doubled the spikes' sensitivity to Ellman reagent (Table 3). Thus, this cysteine 1163 generates a target for reagent-mediated inhibition, even when it is present within the context of the MHV A59 S2 domains.

DISCUSSION

To examine MHV spike-mediated fusion, the thiol blocker Ellman reagent was used to modify the spike structure, and then either virions or cDNA-expressed spikes were tested for infectivity or fusion potency in quantitative assays. The reagent specifically inactivated the infectivity of MHV (strain JHM) virions by eliminating their ability to mediate virion-cell fusion. The inactivation required that the spikes be at a physiological temperature, thereby permitting thermally induced exposure of reactive thiols. The reagent failed to inhibit MHV (strain A59) infectivity, presumably because it lacks an unpaired cysteine in the spike protein.

Ellman reagent also blocked intercellular fusion induced by vaccinia virus-expressed S proteins. Its ability to inhibit this intercellular fusion was considerably less dramatic than that seen with virions but was potent enough to test site-directed cysteine mutants of S protein for their sensitivity to reagent exposure. The reagent was most efficient at blocking fusion of those spikes with a cysteine residue (Cys-1163) lying within the integral membrane S2 spike fragment.

Given the present data, the most reasonable interpretation is that Cys-1163 is a reactive thiol that is exposed at a physiological temperature and then targeted by Ellman reagent for nitrothiobenzoate modification. However, it is known that single-amino-acid changes in the MHV spike can alter structure at more than one portion of the polypeptide chain. Indeed, a series of point mutations in S2 that lie within 100 residues of Cys-1163 confer resistance to neutralization by an S1-binding monoclonal antibody (20). Therefore, it is conceivable that mutations at codon 1163 result in relatively dramatic changes in protein structure such that one or more of the other thiols in S1 or S2 are rendered available for modification. There is clearly a need for further biochemical studies to identify the S peptide fragments that are modified by Ellman reagent. Sequence analyses of spike genes from variants of MHV (strain JHM) selected for resistance to Ellman reagent may also help to identify the target of modification.

Cysteine blockade did not affect S binding to cellular receptor but did prevent the further structural changes in the protein that are required for fusion function. This brings up the question of what kinds of further conformational changes might be blocked. One obvious point of discussion concerns the role of disulfide rearrangements in the obligate structural transitions. Ellman reagent blocks human immunodeficiency virus and Sindbis virus solely at the penetration stage of infection, and this has been taken as evidence of disulfide rearrangement during the fusion event (1, 32). Similar attempts to use Ellman reagent to prevent penetration of MHV particles that had been previously adsorbed to receptor-bearing cells were unsuccessful, perhaps because the fusion process is very rapid relative to thiol reactivity. In addition, attempts to enhance MHV penetration by exogenous addition of reducing agents were similarly unsuccessful (data not shown). It is also quite obvious that fusion mediated by MHV spikes can occur regardless of whether the S2 ectodomain contains 12 or 13 cysteines—both A59 and JHM strains induce pH-independent fusion. Thus, there is little evidence that the JHM-specific Cys-1163 is

TABLE 3. Y1163C change in the hybrid spike protein $S1_4$:$S2_{A59}$ increases sensitivity to Ellman reagent[a]

Plasmid	β-Galactosidase activity (ng/50 μl)		% Inhibition
	+ Ellman reagent	− Ellman reagent	
Expt 1			
pTM1 (no S) (negative control)	0.046	0.051	
pTM1-$S1_4$:$S2_{A59}$ 1	0.156	0.209	30
pTM1-$S1_4$:$S2_{A59}$ 2	0.126	0.151	20
pTM1-$S1_4$:$S2_{A59}$ (Y1163C) 1	0.125	0.221	54
pTM1-$S1_4$:$S2_{A59}$ (Y1163C) 2	0.118	0.181	45
pG1NT7-β-gal (positive control)	27.94	29.16	4
Expt 2			
pTM1 (no S) (negative control)	0.048	0.054	
pTM1-$S1_4$:$S2_{A59}$ 1	0.175	0.215	21
pTM1-$S1_4$:$S2_{A59}$ 2	0.162	0.212	29
pTM1-$S1_4$:$S2_{A59}$ (Y1163C) 1	0.128	0.206	47
pTM1-$S1_4$:$S2_{A59}$ (Y1163C) 2	0.108	0.186	55
pG1NT7-βgal (positive control)	6.62	7.53	12

[a] Relative fusion potential of the expressed spike proteins was assessed by the β-galactosidase reporter gene activation assay as described in the footnotes to Table 2.

needed to participate in a novel disulfide exchange that then leads to a structure competent to induce membrane fusion.

Appeals for a type of conformational change independent of novel disulfide formation could be made if one assumes that the coronavirus spike bears structural similarities to that of influenza hemagglutinin (HA). Indeed, the stalk-like appearance of the spike oligomer in electron micrographs (6), along with its two predicted amphipathic helix domains (5, 7) (Fig. 3), suggests that its high-resolution structure might be modeled after that of the influenza virus HA. Detailed structural comparison of the fusion-inactive and fusion-active conformers of HA has revealed a remarkable transition in the peptide spanning its two helical regions. In HA, this region converts from a monomeric, noncoiled structure to a triple-stranded coiled coil upon exposure to fusion-activating acidic conditions (2, 3). This transition links the helices of the inactive HA into an extended coil structure suitable for inducing fusion. Support for an analagous conformational change in the human immunodeficiency virus fusion process was recently demonstrated by correlating coil-disrupting gp41 mutations with reduced fusion (41). Primary sequence data place the Cys-1163 of S2 near the middle of a 150-residue stretch of peptide linking two predicted alpha helical domains (Fig. 3). Thus, a dramatic conformational change in this stretch of S2 might be required to generate oligomeric helical coiled coils, and such change is not possible with Ellman reagent-modified Cys-1163. It must be noted, however, that the 10 helix-breaking prolines in this connecting region make it improbable that it could itself form a coiled coil and thereby link the two heptad domains of S2 in a manner analogous to the HA conformational change.

Finally, one cannot ignore the possibility that the Ellman reagent modification destroys a directly acting fusion peptide domain. On the MHV spike, a fusion peptide domain has not yet been identified. The fusion domain is not liable to be adjacent to the S1-S2 cleavage site, as one might expect it to be on the basis of its position in the fusion proteins of many other viruses (40). This is because the amino terminus of S2 formed by proteolysis of the spike precursor is not hydrophobic and the spike precursor cleavage is not required for fusion activation (34, 38). Thus, it is possible that the mildly hydrophobic residues spanning Cys-1163 (Tyr–Gly–Leu–Cys-1163–Phe–Ile–His–Phe) could act directly as a membrane-intercalating fusion peptide. If so, modification of Cys-1163 by Ellman reagent would surely disrupt fusion function.

ACKNOWLEDGMENTS

I thank Eric Hunter (University of Alabama at Birmingham), Dennis Brown (University of Texas at Austin), and Hans-Martin Jäck (Loyola University Medical Center) for encouraging comments and suggestions during the course of this work. Thanks also go to Edward Berger and Bernard Moss (National Institutes of Health) for providing vaccinia virus recombinant vTF7.3 and plasmid pG1NT7-βgal, to Manfred Gossen and Herman Bujard (University of Heidelberg, Heidelberg, Germany) for the HeLa-tTA cells and pUHD10-3 expression vector, to Kathryn Holmes (University of Colorado, Denver) for antireceptor antibody CC1, and to Michael Buchmeier (Scripps Research Institute) for antipeptide antibodies directed against receptor and spike proteins.

This work was supported by NIH grant R29-NS-31616 and by a grant from the Schweppe Foundation of Chicago.

REFERENCES

1. **Abell, B. A., and D. T. Brown.** 1993. Sindbis virus membrane fusion is mediated by reduction of glycoprotein disulfide bridges at the cell surface. J. Virol. **67:**5496–5501.
2. **Bullough, P. A., F. M. Hughson, J. J. Skehel, and D. C. Wiley.** 1994. Structure of influenza haemagglutinin at the pH of membrane fusion. Nature (London) **371:**37–43.
3. **Carr, C. M., and P. S. Kim.** 1993. A spring-loaded mechanism for the conformational change of influenza hemagglutinin. Cell **73:**823–832.
4. **Cavanagh, D.** 1995. The coronavirus surface glycoprotein. *In* S. G. Siddell (ed.), The Coronaviridae. Plenum Press, New York.
5. **Chambers, P., C. R. Pringle, and A. J. Easton.** 1990. Heptad repeat sequences are located adjacent to hydrophobic regions in several types of virus fusion glycoproteins. J. Gen. Virol. **71:**3075–3080.
6. **Davies, H. A., and M. R. Macnaughton.** 1979. Comparison of the morphology of three coronaviruses. Arch. Virol. **59:**25–33.
7. **de Groot, R. J., W. Luytjes, M. C. Horzinek, B. A. M. van der Zeijst, W. J. M. Spaan, and J. A. Lenstra.** 1987. Evidence for a coiled-coil structure in the spike proteins of coronaviruses. J. Mol. Biol. **196:**963–966.
8. **Delmas, B., and H. Laude.** 1990. Assembly of coronavirus spike protein into trimers and its role in epitope expression. J. Virol. **64:**5367–5375.
9. **Doms, R. W.** 1993. Protein conformational changes in virus-cell fusion. Methods Enzymol. **221:**61–72.
10. **Dveksler, G. S., M. N. Pensiero, C. B. Cardellichio, R. K. Williams, G.-S. Jiang, K. V. Holmes, and C. W. Dieffenbach.** 1991. Cloning of the mouse hepatitis virus (MHV) receptor: expression in human and hamster cell lines confers susceptibility to MHV. J. Virol. **65:**6881–6891.
11. **Dveksler, G. S., M. N. Pensiero, C. W. Dieffenbach, C. B. Cardellichio, A. A. Basile, P. E. Elia, and K. V. Holmes.** 1993. Mouse coronavirus MHV-A59 and blocking anti-receptor monoclonal antibody bind to the N-terminal domain of cellular receptor MHVR. Proc. Natl. Acad. Sci. USA **90:**1716–1720.
12. **Elroy-Stein, O., and B. Moss.** 1990. Cytoplasmic expression system based on constitutive synthesis of bacteriophage T7 RNA polymerase in mammalian cells. Proc. Natl. Acad. Sci. USA **87:**6743–6747.
13. **Falkner, F. G., and B. Moss.** 1988. *Escherichia coli gpt* gene provides dominant selection for vaccinia virus open reading frame expression vectors. J. Virol. **62:**1849–1854.
14. **Fuerst, T. R., P. L. Earl, and B. Moss.** 1987. Use of a hybrid vaccinia virus-T7 RNA polymerase system for expression of target genes. Mol. Cell. Biol. **7:**2538–2544.
15. **Fuerst, T. R., E. G. Niles, F. W. Studier, and B. Moss.** 1986. Eukaryotic transient expression system based on recombinant vaccinia virus that synthesizes bacteriophage T7 RNA polymerase. Proc. Natl. Acad. Sci. USA **83:**8122–8126.
16. **Gallagher, T. M.** 1995. Overexpression of the MHV receptor: effect on progeny virus secretion. Adv. Exp. Med. Biol. **380:**331–336.
17. **Gallagher, T. M., C. Escarmis, and M. J. Buchmeier.** 1991. Alteration of the pH dependence of coronavirus-induced cell fusion: effect of mutations in the spike glycoprotein. J. Virol. **65:**1916–1928.
18. **Gallagher, T. M., S. E. Parker, and M. J. Buchmeier.** 1990. Neutralization-resistant variants of a neurotropic coronavirus are generated by deletions within the amino-terminal half of the spike glycoprotein. J. Virol. **64:**731–741.
19. **Gossen, M., and H. Bujard.** 1992. Tight control of gene expression on mammalian cells by tetracycline-responsive promoters. Proc. Natl. Acad. Sci. USA **89:**5547–5551.
20. **Grosse, B., and S. G. Siddell.** 1994. Single amino acid changes in the S2 subunit of the MHV surface glycoprotein confer resistance to neutralization by S1 subunit-specific monoclonal antibody. Virology **202:**814–824.
21. **Hirano, N., T. Murakami, K. Fujiwara, and M. Matsumoto.** 1978. Utility of mouse cell line DBT for propagation and assay of mouse hepatitis virus. Jpn. J. Exp. Med. **48:**71–75.
22. **Innis, M. A., and D. H. Gelfand.** 1990. Optimization of PCRs, p. 3–12. *In* M. A. Innis, D. H. Gelfand, J. J. Sninsky, and T. J. White (ed.), PCR protocols. Academic Press, Inc., San Diego, Calif.
23. **Kawasaki, E. S.** 1990. Amplification of RNA, p. 21–27. *In* M. A. Innis, D. H. Gelfand, J. J. Sninsky, and T. J. White (ed.), PCR protocols. Academic Press, Inc., San Diego, Calif.
24. **Klausner, R. D., J. G. Donaldson, and J. Lippincott-Schwartz.** 1992. Brefeldin A: insights into the control of membrane traffic and organelle structure. J. Cell Biol. **116:**1071–1080.
25. **Luytjes, W., L. S. Sturman, P. J. Bredenbeek, J. Charik, B. A. M. van der Zeijst, M. C. Horzinek, and W. J. M. Spaan.** 1987. Primary structure of the glycoprotein E2 of coronavirus MHV-A59 and identification of the trypsin cleavage site. Virology **161:**479–487.
26. **Moss, B., O. Elroy-Stein, T. Mizukami, W. A. Alexander, and T. R. Fuerst.** 1990. New mammalian expression vectors. Nature (London) **348:**91–92.
27. **Nussbaum, O., C. C. Broder, and E. A. Berger.** 1994. Fusogenic mechanisms of enveloped-virus glycoproteins analyzed by a novel recombinant vaccinia virus-based assay quantitating cell fusion-dependent reporter gene activation. J. Virol. **68:**5411–5422.
28. **Opstelten, D.-J. E., P. de Groote, M. C. Horzinek, H. Vennema, and P. J. M. Rottier.** 1993. Disulfide bonds in folding and transport of mouse hepatitis coronavirus glycoproteins. J. Virol. **67:**7394–7401.
29. **Parker, S. E., T. M. Gallagher, and M. J. Buchmeier.** 1989. Sequence analysis reveals extensive polymorphism and evidence of deletions within the E2 glycoprotein of several strains of murine hepatitis virus. Virology **173:**664–673.
30. **Rey, F. A., F. X. Heinz, C. Mandl, C. Kunz, and S. C. Harrison.** 1995. The

envelope glycoprotein from tick-borne encephalitis virus at 2 A resolution. Nature (London) **375:**291–298.
31. **Riddles, P. W., R. L. Blakeley, and B. Zerner.** 1979. Ellman's reagent: 5,5′-dithiobis(2-nitrobenzoic acid)—a reexamination. Anal. Biochem. **94:**75–81.
32. **Ryser, H. J.-P., E. M. Levy, R. Mandel, and G. J. DiSciullo.** 1994. Inhibition of human immunodeficiency virus infection by agents that interfere with thiol-disulfide interchange upon virus-receptor interaction. Proc. Natl. Acad. Sci. USA **91:**4559–4563.
33. **Sambrook, J., E. F. Fritsch, and T. Maniatis.** 1989. Molecular cloning: a laboratory manual, 2nd ed. Cold Spring Harbor Laboratory, Cold Spring Harbor, N.Y.
34. **Stauber, R., M. Pfleiderara, and S. Siddell.** 1993. Proteolytic cleavage of the murine coronavirus surface glycoprotein is not required for fusion activity. J. Gen. Virol. **74:**183–191.
35. **Sturman, L. S., C. S. Ricard, and K. V. Holmes.** 1985. Proteolytic cleavage of the E2 glycoprotein of murine coronavirus: activation of cell-fusing activity of virions by trypsin and separation of two different 90K cleavage fragments. J. Virol. **56:**904–911.
36. **Sturman, L. S., C. S. Ricard, and K. V. Holmes.** 1990. Conformational change of the coronavirus peplomer glycoprotein at pH 8.0 and 37°C correlates with virus aggregation and virus-induced cell fusion. J. Virol. **64:**3042–3050.
37. **Sturman, L. S., and K. K. Takemoto.** 1972. Enhanced growth of a murine coronavirus in transformed mouse cells. Infect. Immun. **6:**501–507.
38. **Taguchi, F.** 1993. Fusion formation by the uncleaved spike protein of murine coronavirus JHMV variant cl-2. J. Virol. **67:**1195–1202.
39. **Taguchi, F.** 1995. The S2 subunit of the murine coronavirus spike protein is not involved in receptor binding. J. Virol. **69:**7260–7263.
40. **White, J. M.** 1992. Membrane fusion. Science **258:**917–924.
41. **Wild, C., J. J. Dubay, T. Greenwell, T. Baird, Jr., T. G. Oas, C. McDanal, E. Hunter, and T. Matthews.** 1994. Propensity for a leucine zipper-like domain of human immunodeficiency virus type 1 gp41 to form oligomers correlates with a role in virus-induced fusion rather than assembly of the glycoprotein complex. Proc. Natl. Acad. Sci. USA **91:**12676–12680.
42. **Williams, R. K., G.-S. Jiang, S. W. Snyder, M. F. Frana, and K. V. Holmes.** 1990. Purification of the 110-kilodalton glycoprotein receptor for mouse hepatitis virus (MHV)-A59 from mouse liver and identification of a nonfunctional, homologous protein in MHV-resistant SJL/J mice. J. Virol. **64:**3817–3823.
43. **Wilson, I. A., J. J. Skehel, and D. C. Wiley.** 1981. Structure of the hemagglutinin membrane glycoprotein of influenza virus at 3 A resolution. Nature (London) **289:**366–373.
44. **Yoo, D., M. D. Parker, and L. A. Babiuk.** 1991. The S2 subunit of the spike glycoprotein of bovine coronavirus mediates membrane fusion in insect cells. Virology **180:**395–399.